

Degradation of poly(vinyl alcohol)-graft-lactic acid copolymers by *Trichotecium roseum* fungus

Rodica Lipsa, Nita Tudorachi, Vasile Cristian Grigoraş, Cornelia Vasile

"Petru Poni" Institute of Macromolecular Chemistry, Gr. Ghica Voda Alley, 41A, 700487, Iasi, Romania

Correspondence to: N. Tudorachi (E-mail: tudorachinita@yahoo.com)

ABSTRACT: The biodegradation of poly(vinyl alcohol) and poly(vinyl alcohol)-graft-lactic acid copolymers was analyzed, using *Trichotecium roseum* fungus. The samples were examined during biodegradation at different periods of exposure. Structural modifications of the biodegraded samples were investigated by Fourier transform infrared-attenuated total reflectance spectroscopy, and the surface morphology was investigated by scanning electron microscopy. The static light scattering results concluded that the weight average molecular mass (M_w) of the copolymers increased after biodegradation, because the fractions with low molecular weight of the copolymers were destroyed. The thermal behavior and stability of the samples before and after the biodegradation period were investigated by differential scanning calorimetry (DSC) and thermogravimetric analyses. The thermogravimetric analyses and their derivatives (TG-DTG) showed that the thermal stability of the biodegraded samples was more raised comparatively to the unbiodegraded ones. The DSC results demonstrated that biodegradation took place in the amorphous domains of the investigated polymer samples and the crystallinity degree increased after 24 biodegradation days. © 2014 Wiley Periodicals, Inc. *J. Appl. Polym. Sci.* **2015**, *132*, 41777.

KEYWORDS: biodegradable; copolymers; grafting; thermal properties

Received 17 September 2014; accepted 17 November 2014

DOI: 10.1002/app.41777

INTRODUCTION

The environmental pollution determined by synthetic polymers has dangerous proportions especially in developed countries, consequently biodegradable polymers have become of great interest.¹ These polymers represent a very good alternative to non-degradable plastics in different applications, such as: packaging, agriculture, pharmaceuticals, and medicine. Biodegradation is a chemical degradation of materials, caused by the action of microorganisms: bacteria, fungi, or algae that determines changes in the chemical structure, loss of mechanical and structural properties, and finally resulting compounds such as water, carbon dioxide, minerals, and intermediate products like biomass and humic materials.² The biodegradation involves several steps: biodeterioration, biofragmentation, assimilation, and mineralization. The high molecular weight and entanglements of polymer chains, however, retard the biodegradation and aging processes of materials.³ The chemical structure of polymers, responsible for functional groups stability, reactivity, hydrophilicity, and swelling behavior, is the most important factor affecting biodegradability.^{4,5} It also depends on environmental factors such as: temperature, moisture, oxygen, pH, and microorganism's consortium.⁶ It was concluded that the biodegradation of polymers is accelerated by the hydrophilicity of the main chain, reduced crystallinity, and the presence of additives. Other important factors that influence

the biodegradability of polymers are the physico-chemical, thermal, and mechanical properties: molecular weight, morphology, glass transition temperature, crystalline surface areas, porosity, and elasticity. Heterochain polymers, particularly those containing oxygen and/or nitrogen atoms in the main chain are the most susceptible to biodegradation and the biodegradation rate increases in the order: ester > carbonate > ether > amide > urea > urethane.

Poly(vinyl alcohol) (PVA) is a synthetic water soluble polymer, with a very broad range of applications: adhesive for paper, wood, textile and leather, finishing agent, emulsifier, and photosensitive coating. The main biomedical uses of PVA are in soft contact lenses, eye drops, embolization particles, tissue adhesion barriers, and as artificial cartilage and meniscus. This large area of applications is due to its very good physico-chemical properties (flexibility, transparency, toughness, and low permeability), biodegradability, biocompatibility non-toxicity, non-carcinogenicity, and low-cost.⁷ The basic properties of PVA are much dependent on the degree of polymerization (DP), degree of hydrolysis (DS), distribution of hydroxyl groups, stereoregularity, and crystallinity. As conventional PVA cannot be processed by traditional technologies, since it decomposes close to its melting point (T_m about 230°C) and has a poor water resistance, various physical⁸⁻¹⁰ or chemical modification¹¹ were achieved to functionality and control the biodegradability and biocompatibility

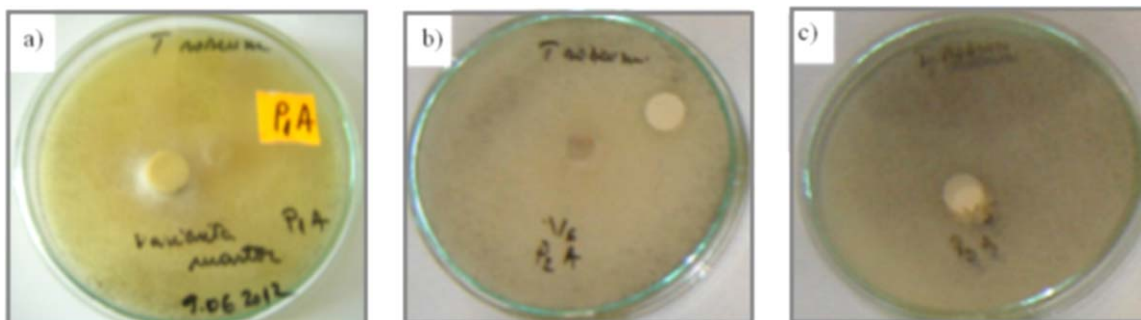


Figure 1. Images of the unbiodegraded samples: (a) PVA; (b) PVA-g-LA (1/1); (c) PVA-g-LA (2.2/1). [Color figure can be viewed in the online issue, which is available at wileyonlinelibrary.com.]

for single or multi-reflection ATR. The ATR crystal plate is made of diamond (1.8 mm diameter) and the solid materials can be put into intimate physical contact with the sampling area through high-pressure clamping, yielding high-quality, and reproducible spectra.

Scanning electron microscopy (SEM) was conducted, using a SEM/ESEM-Edax-Quanta 200, equipped with a large field detector. The acceleration voltage was 20 kV, under low vacuum mode, 60–100 Pa. After incubation with fungal cultures, the copolymer samples were taken out from the culture and repeatedly rinsed with distilled water, dried at 30°C, and used for evaluation of the biodegradation efficiency. Micrographs of the samples were recorded at different magnifications to observe the modification of the samples surface, during the biodegradation process.

Static light scattering (SLS) measurements were achieved in “batch mode” using a DAWN-DSP photometer (Wyatt Tech.), equipped with a HeNe laser (633 nm, 5 mW). This detector was calibrated with toluene and normalized with aqueous solution of PEG 6430, filtered through a crucible with 0.2 μm pores. The light scattering intensities were recorded at 18 angles between 14° ÷ 152°. The laser light scattering data processing and calculations of weight-average molecular weight (M_w), radius of gyration (R_g), and second virial coefficient (A_2) were achieved by Astra 4.90.07 software, according to Zimm procedure. The Zimm plots were computed using Berry formalism [eq. (1)].

$$\left(\frac{K_c}{R\theta}\right)^{0.5} \text{ versus } \sin^2\left(\frac{\theta}{2}\right) \quad (1)$$

The “batch mode SLS” measurements for the 90° angle detector were processed in accordance with Berry formalism to construct the Debye plots and extract the averaged values (for ten points from the recorded intensity slice) of M_w and R_g for each polymer dilution. The values of the refractive index increments, d_n/d_c were determined by differential refractometry using an Optilab-rEX refractometer from Wyatt Technology (Santa Barbara, CA). The measurements were achieved in off-line mode at 25°C and 633 nm. For the differential refractometry and light scattering experiments, the stock and diluted solutions in the range of $8E^{-4}$ – $8E^{-5}$ g/mL (for PVA and PVA-g-LA copolymers) were prepared, in salted aqueous solutions (0.5M NaCl, in deionized water). All the solvents were filtered through 0.02 μm

Anotop filters (Whatman). Before the dilution stage, every stock sample was filtered through the membrane filter, with 0.8 μm pore size. Then, the solutions were transferred into cylindrical quartz glass scattering cells (Quartz SUPRASIL, Hellma GmbH & Co. KG, Germany), immediately sealed with plastic caps, and kept 2 days for degassing.

Differential scanning calorimetry (DSC) analysis was carried out by means of a power compensated calorimeter Pyris Diamond (Perkin Elmer). The samples, with weight ranging from 7 to 7.5 mg were kept in the cell at 120°C, for 5 minutes to remove the water traces. Then, they were quenched at 10°C and performed at least twice in the temperature range 10°C–240°C, with a heating rate of 10°C/min and a nitrogen flow of 20 mL/min. The device was calibrated for temperature and energy, using pure indium as standard. The T_g values were determined from the second heating DSC scan. The samples were heated in an open Al₂O₃ crucible and Al₂O₃ as reference material was used.

Thermogravimetric analyses (TGA) of the copolymers were performed by means of a STA 449 F1 Jupiter thermobalance (Netzsch-Germany). The samples, with a mass ranging from 7 to 10 mg were heated from 30°C to 600°C, with a heating rate of 10°C/min. Nitrogen gas (99.99% purity), as carrier with flow rate of 50 mL/min was used. The samples were heated in open Al₂O₃ crucible and Al₂O₃ as reference material was used. The data collection was carried out with Proteus® software.

RESULTS AND DISCUSSION

Biodegradation Test

Samples of PVA and PVA-g-LA copolymers at two molar ratios PVA/LA (1/1 and 2.2/1), as disks with diameter of 10 mm and 1 mm thickness, were biodegraded with *T. roseum* fungus and the clear zone diameter was measured according to the literature methods.²³ In Figure 1 are shown images of PVA and PVA-g-LA copolymers, before inoculation with *T. roseum* fungus. The visual aspect of the fungi on the copolymer disks surface was monitored during biodegradation, and the physico-chemical and thermal properties of the biodegraded samples, comparatively to the unbiodegraded ones were analyzed after 24 biodegradation days.

During the copolymer samples exposure to biodegradation on the solid medium, it could be observed that hyphae of fungi

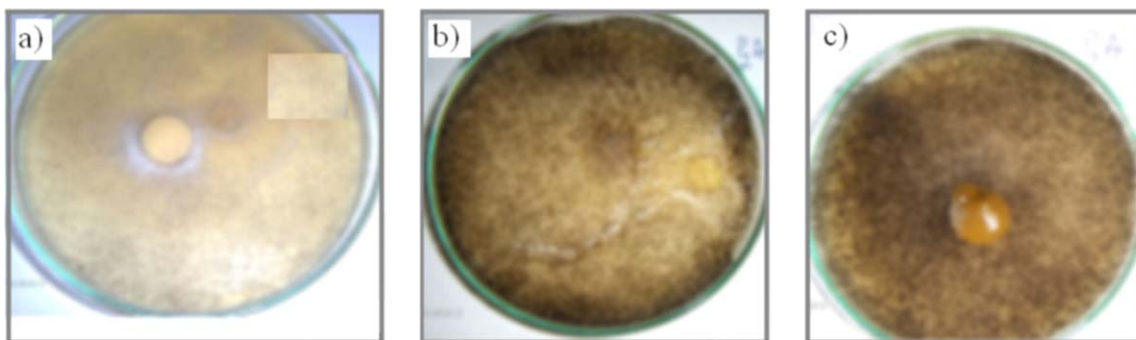


Figure 2. Images of the biodegraded-samples (after six biodegradation days): (a) PVA; (b) PVA-g-LA (1/1); (c) PVA-g-LA (2.2/1). [Color figure can be viewed in the online issue, which is available at wileyonlinelibrary.com.]

grew on the copolymer surface, even in the first 6 days of biodegradation (Figure 2), with the formation of a clear halo zone around the colonies and copolymer samples. The fungal attack was faster in the case of PVA-g-LA (1/1) copolymer that contains more lactic acid units in its structure, as well as in PVA-g-LA (2.2/1) copolymer. This affirmation is based on the values of the clear zone diameter: 35 mm (PVA/LA = 1/1) and 20 mm (PVA/LA = 2.2/1), respectively, after six biodegradation days. In the case of PVA, the presence of fungi on the agar medium is reduced and the clear zone diameter is 10 mm. Subsequently, the fungus reached maturity and the formed spores attack was much more aggressive. An abundant growth of fungi on the PVA-g-LA copolymers surface after 24 biodegradation days, was observed (Figure 3), when the hyphae covered approximately 90% of the surface. This time a more advanced biodegradation of the copolymer disks could be noticed, that occurred by disappearance of the sample fragments and even a process of dissolution started, determined by the culture medium humidity. The biodegraded samples, were then repeatedly rinsed with distilled water, the fungus being carefully removed, dried by lyophilization at -50°C and vacuum of 13 Pa, and used for characterization.

FTIR Characterization

The FTIR-ATR spectra of PVA and PVA-g-LA copolymers, unbiodegraded and biodegraded are represented in Figure 4. In the FTIR-ATR spectrum of the biodegraded PVA can be observed that not significant modifications appeared, compar-

tively to unbiodegraded PVA. Many absorption bands, in unbiodegraded PVA spectrum are also noticed in the spectrum of biodegraded PVA, but slightly shifted: at 3276 cm^{-1} (in the unbiodegraded PVA) and 3263 cm^{-1} (in the biodegraded PVA) are recorded νOH stretching vibrations of the hydroxyl groups and intermolecular hydrogen linkages in polyols, at 2913, 1417 cm^{-1} (in the unbiodegraded PVA) and 2909, 1418 cm^{-1} (in the biodegraded PVA) are recorded the stretching vibrations νCH_2 and δCH_2 , characteristic to methylene groups in the polymer. The signals at 1087 cm^{-1} (in the unbiodegraded PVA) and 1079 cm^{-1} (in the biodegraded PVA) are characteristic to $\nu\text{C}-\text{OH}$ stretching vibrations of the secondary alcohols. However, it can be noticed that in the PVA biodegraded spectrum some absorption peaks disappeared (at 1707, 1566, and 1136 cm^{-1}), characteristic to νCO stretching vibrations of the residual acetyl groups COOCH_3 and $\nu\text{C}-\text{OH}$ in secondary alcohols. This result suggests that by fungal attack, the residual acetyl groups existent in PVA (νCO from COOCH_3) and $\text{CH}-\text{OH}$ linkages were destroyed, being in accordance with the literature data.²⁴ The enzyme release from microorganisms would accelerate the material degradation. The microorganisms are able to determine the enzymatic degradation of polymers, this is the main biodegradation process for several medical polymers, that is, polyurethane.²⁵ It has been reported that many fungi develop powerful enzyme systems to degrade highly stable polymers. These enzyme systems promote the reduction of peroxides to free radicals. Fungal hyphae can penetrate into the polymer, influencing the mechanical stability and facilitate water diffusion

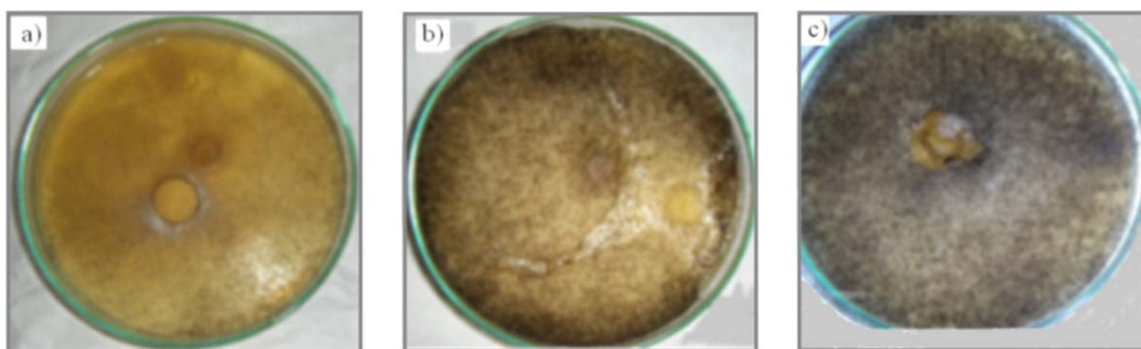


Figure 3. Images of the biodegraded samples (after 24 biodegradation days): (a) PVA; (b) PVA-g-LA (1/1); (c) PVA-g-LA (2.2/1). [Color figure can be viewed in the online issue, which is available at wileyonlinelibrary.com.]

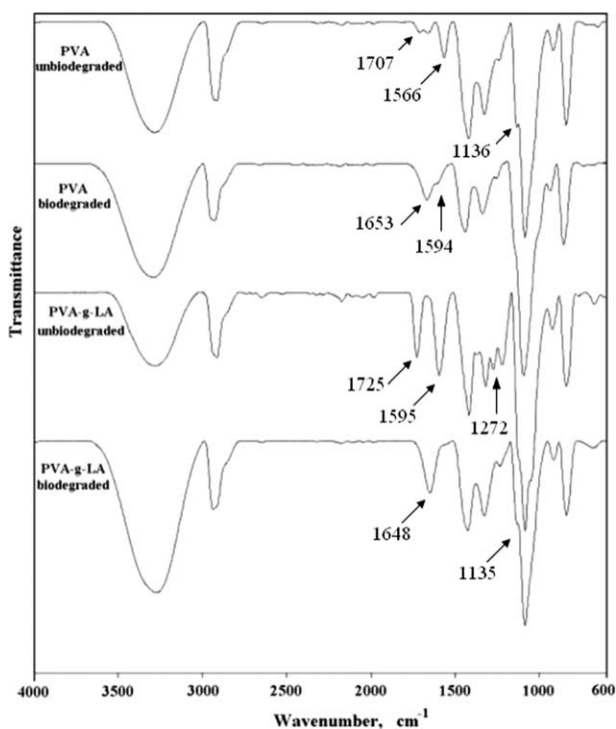


Figure 4. FTIR spectra of PVA and PVA-g-LA copolymers, before and after 24 biodegradation days by *Trichotectium roseum* fungus.

into the material. Hyphal penetration provides mechanical degradation as a complement to chemical breakdown.^{26,27} Consequently, in the biodegraded copolymer some new absorption bands appeared at 1653 and 1594 cm^{-1} characteristic to $\nu\text{C}=\text{O}$ and δNH stretching vibrations of the amide I and amide II groups, resulting from the protein production by microorganisms growth (*Trichotectium roseum*).

In the FTIR-ATR spectrum of PVA-g-LA biodegraded sample (Figure 4), some new absorption bands appeared (at 1648 and 1135 cm^{-1}) and other absorption bands recorded at 1725, 1595, and 1272 cm^{-1} (in the unbiodegraded sample) disappeared. The stretching vibrations $\nu\text{C}=\text{O}$ of the ester groups recorded at 1725 and 1272 cm^{-1} and the stretching vibration $\nu\text{C}=\text{O}$ of the COO^- groups recorded at 1595 cm^{-1} in the unbiodegraded copolymer disappeared, suggesting the scission of these groups by biodegradation. The new absorption bands in the biodegraded copolymer at 1648 and 1135 cm^{-1} are assigned to νCO stretching vibration of the peptide and ester bonds existent in *T. roseum* fungus. This result can be explained, as the ester groups are broken by hydrolytic scission caused by the microorganisms existent in the environment.²⁸

Scanning Electron Microscopy

The SEM micrographs of PVA and PVA-g-LA copolymers (unbiodegraded and biodegraded samples), are represented in Figure 5. In the SEM micrographs of the biodegraded samples [Figure 5(b,d,f)] can be noticed an ample colonization of fungi on the surface. The attachment and formation mechanism of biofilms on the surfaces is a very complex phenomenon. In the main it is based on colloid chemistry and surface-surface interactions, where the adhesion strength depends on short and long

range interactions (Van der Waals forces, hydrogen bonding, electrostatic interactions, etc.).²⁹ After the cell attachment, the biofilm formation begins by colonization and production of extracellular polymer substance that embeds the microorganisms, ensures the adhesion to the surface, and protects the biofilm by the outer environment. The extracellular polymer substance provides stability to the biofilm and protection against antimicrobial agents, which in turn causes initiation and propagation of the material degradation. Consequently, on the biodegraded PVA surface can be observed the appearance of tiny holes; in the case of biodegraded PVA-g-LA copolymers several large holes and cracks appeared that penetrated deep into sample, also in the biodegraded PVA-g-LA copolymer the disappearance of some polymer fragments was noticed. In the case of the biodegraded copolymers the biodegradation degree was influenced by the molar ratio PVA/LA. The PVA-g-LA copolymer, with molar ratio 1/1 [Figure 5(d)] presents an advanced biodegradation and some weight losses caused by degradation of the fragments with lower molecular weights. The presence of the ester groups in the copolymers determines the biodegradation degree improve, comparatively to PVA. For all the studied samples it was observed an abundant growth of fungi at the end of the biodegradation time (24 days), when the surface was covered almost 70%–90% with fungi.

SLS Characterization

The light scattering methods allow the exploration of different associations of biomacromolecules and require suitable solvents for the molecular dissolution of the components.³⁰ The refractometric and SLS measurements were made on unfractionated samples (unbiodegraded and biodegraded polymers), which were kept 2 days for degassing in scintillation vials. This method requires knowledge of the specific refractive index increments (d_n/d_c of the sample/solvent combination used), in order to determine the molecular weight values and characteristic parameters (weight-average molecular weight \bar{M}_w , radius of gyration R_g , and second virial coefficient A_2). The values of d_n/d_c are dependent on the measurement temperature, solvent type, wavelength of incident light, solution concentration, and molecular weight of the polymer.^{31,32} Laser light scattering of macromolecular compounds was described by Zimm [eq. (2)].

$$\frac{K_c}{R_\theta} = \frac{1}{\bar{M}_w} + 2A_2c + \frac{16\pi^2 R_g^2}{3\lambda_0 \bar{M}_w} \sin^2 \frac{\theta}{2} + \dots \quad (2)$$

with:

$$K = \frac{4\pi^2 (d_n/d_c)^2 n^2}{N\lambda_0^4}$$

where, K is the optical constant for vertically polarized incident light, c is concentration (g/mL) of the scattering species in solution, R_θ is the Rayleigh ratio (directly proportional to the ratio of the scattered light intensity at angle θ and the incident light intensity), N is the Avogadro number, n solution refractive index, and λ_0 is the wavelength of the incident light. In the following calculations, it is assumed that the concentration is sufficiently low to neglect the terms containing the more raised virial coefficients than A_2 . The R_g value can be found from the initial slope of a plot K_c/R_θ versus $\sin^2(\theta/2)$ and $1/\bar{M}_w$ from the

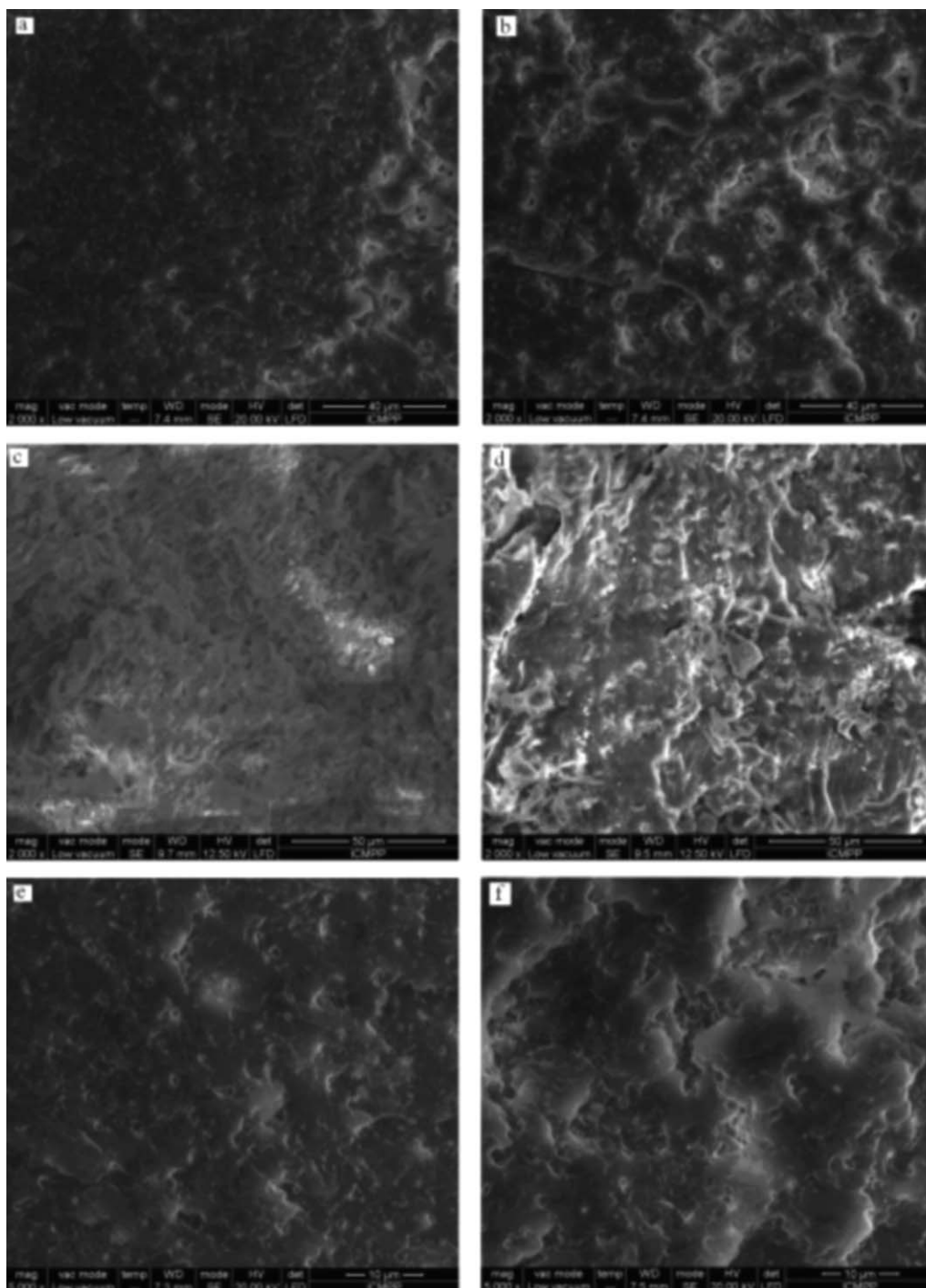


Figure 5. SEM micrographs: (a) PVA; (c) PVA-g-LA (1/1); (e) PVA-g-LA (2.2/1) (before biodegradation); (b) PVA; (d) PVA-g-LA (1/1); (f) PVA-g-LA (2.2/1) (after 24 biodegradation days).

intersection of the curve with the ordinate. The second virial coefficient A_2 is an important parameter that quantitatively characterizes the thermodynamic interaction between the solute molecules at a specific temperature. The polymer-solvent interactions dominate the polymer-polymer interactions when $A_2 > 0$.³³ In Table I are given the values of d_n/d_o , M_w , R_g , and A_2 for the unbiodegraded and biodegraded samples. The presented data demonstrate that the biodegraded samples have a more

raised average weight molecular weight (\bar{M}_w), compared with the unbiodegraded ones. These results suggest that by biodegradation in the presence of *T. roseum* fungus, the low molecular weight macromolecular chains were destroyed, as reported in literature.³⁴ Also, in the case of biodegraded samples possible intermolecular interactions dominate to the detriment of intramolecular ones. In the copolymer-solvent systems, a competition between these interactions exists, which was caused by the

Table I. SLS Analyses of PVA and PVA-g-LA Copolymers After 24 Days of Biodegradation with *Trichotecium roseum* Fungus

Sample	PVA/LA molar ratio	d_n/d_c (mL/g)	R_g (nm)	$\bar{M}_w \times 10^{-5}$ (g/mol)	$A_2 \times 10^4$ mol mL/g ²
PVA unbiodegraded	1/0	0.153	110.7	35.39	6.943
PVA biodegraded	1/0	0.150	ND	45.08	7.043
PVA-g-LA unbiodegraded	1/1	0.149	ND	13.49	7.868
PVA-g-LA biodegraded	1/1	0.144	ND	22.75	6.828
PVA-g-LA unbiodegraded	2.2/1	0.140	ND	18.37	6.879
PVA-g-LA biodegraded	2.2/1	0.138	ND	25.00	6.292

ND, not detected.

solvent nature, copolymer structure (hydrophilic–hydrophobic balance), and the mixing conditions (temperature, pH, ionic strength).³⁵ The results of the SLS study suggest that by biodegradation the fractions with low molecular weight of PVA and PVA-g-LA copolymers lowered and some were removed, consequently M_w of the biodegraded copolymers increased. This conclusion is also sustained by other literature data.³⁶ The positive values of A_2 , for all unbiodegraded and biodegraded samples

demonstrate the presence of favorable polymer–solvent interactions. Also, the SLS results suggest that water is a good solvent for all the samples ($A_2 > 0$); the decrease of d_n/d_c and increase of \bar{M}_w of the biodegraded samples compared with blanks, suggested that these fungi metabolized a part of the copolymers, consequently the biodegradation process influenced the solution polymer properties.

DSC Analysis

In Figure 6 and Table II are shown the DSC curves and the main thermal characteristics of the unbiodegraded and biodegraded samples. It can be noticed that biodegraded PVA and PVA-g-LA (2.2/1) copolymer have no glass transition temperature (T_g), consequently the heat capacity ΔC_p could not be calculated on 10°C–240°C interval, suggesting that biodegradation affected the amorphous domains. Moreover, it can be observed that the melting temperature (T_m), melting enthalpy (ΔH), and crystallinity degree (X_c) of the biodegraded PVA and copolymers have a raised value comparatively to the unbiodegraded samples. The crystallinity degree indicates the amount of crystalline regions in the polymer, compared with the amorphous ones. On the other hand, it is noticed that the melting domain of biodegraded PVA becomes narrower (53°C) comparatively to 65°C in the case of unbiodegraded PVA, demonstrating that by biodegradation the amorphous–crystalline interface was affected, and the crystallinity degree (58.5%) and crystalline fraction, respectively increased. Also, it can be observed that the T_m value of biodegraded PVA is more raised (229°C), comparatively to the T_m of unbiodegraded PVA (219°C), which supports the idea of crystallinity improvement by biodegradation. In fact, the short macromolecular chains at the crystalline–amorphous interface are biodegraded and consequently the PVA small crystallites which form a quasi-amorphous phase are eliminated. This result is in accordance with the shape of the DSC curve.

The graft PVA-g-LA copolymers have lower glass transition temperatures comparatively to PVA, due to the crystallinity degree and polarity decrease and of the free volume increase. The thermal behavior in the crystalline domain of the copolymers shows wide melting domains (60°C) compared with PVA (Figure 6), suggesting that the newly formed crystallites by grafting, are imperfect and have reduced dimensions. Also, the T_m and ΔH values of unbiodegraded PVA-g-LA (molar ratio PVA/LA 1/1) (186°C, 32.79 J/g) and PVA-g-LA 2.2/1 (185°C, 33.59 J/g) are much lower comparatively to PVA (219°C, 90.01 J/g). The effect

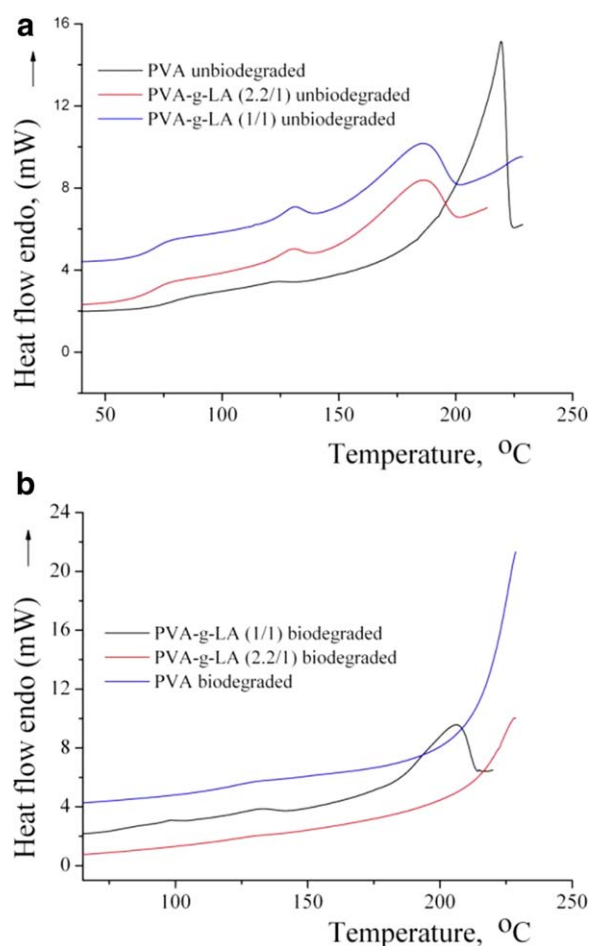


Figure 6. DSC curves of PVA and PVA-g-LA copolymers: (a) unbiodegraded; (b) after 24 biodegradation days by *Trichotecium roseum* fungus. [Color figure can be viewed in the online issue, which is available at wileyonlinelibrary.com.]

Table II. DSC Parameters of PVA and PVA-g-LA Copolymers After 24 Days of Biodegradation with *Trichotecium roseum* Fungus

Sample	PVA/LA molar ratio	T_g (°C)	T_m (°C)	ΔC_p (J/g °C)	ΔH (J/g)	X_c (%)
PVA (blank)	1/0	76	219	0.225	90.01	57.70
PVA (biodegraded)	1/0	-	229	-	91.33	58.54
PVA-g-LA (blank)	1/1	70	186	0.434	32.79	22.94
PVA-g-LA biodegraded	1/1	76	206	0.165	41.82	26.80
PVA-g-LA (blank)	2.2/1	69	185	0.400	33.59	21.53
PVA-g-LA biodegraded	2.2/1	-	228	-	76.10	48.78

of biodegradation on the copolymers is similar to PVA: the amorphous domains were destroyed and the average molecular weight increased, determining the T_g and ΔC_p increase in the case of biodegraded PVA-g-LA copolymer (1/1) (Table II), while these parameters could not be detected in the case of biodegraded PVA-g-LA (2.2/1) copolymer, suggesting that biodegradation affected all the amorphous domains. Concerning the melting process, the biodegradation result on the copolymers is similar: the T_m and ΔH_m values of the biodegraded copolymers are more raised comparatively to the unbiodegraded ones,

demonstrating the disappearance of the amorphous phase and imperfect crystallites by biodegradation. Consequently, the DSC results concluded that by the grafting reaction is facilitated the biodegradation process, which took place in the amorphous domains of the copolymers, also sustained by the X_c values increase. These results are also in accordance with the literature data: the amorphous regions of copolymers are loosely packed, and thereby more susceptible to biodegradation.³⁵

Thermogravimetric Analyses

The thermal behavior of unbiodegraded and biodegraded PVA and PVA-g-LA copolymers, in controlled laboratory conditions in the presence of *T. roseum* fungus, was studied by the TGA, in nitrogen atmosphere, on 30°C–600°C temperature interval, with heating speed of 10°C/min. The TG and DTG curves of PVA and PVA-g-LA copolymers are presented in Figure 7 and the main thermal parameters in Table III. The thermal behavior of unbiodegraded and biodegraded samples is dependent of the chemical structure and molar ratio of the components.

PVA and PVA-g-LA copolymers present three thermal decomposition stages that occur with different speeds, in the case of unbiodegraded and biodegraded samples. In the first degradation stage, the weight losses are reduced (until maximum 6.8 wt %), due to the elimination of bound water molecules. In the second thermal decomposition stage (258°C–385°C) significant weight losses ranging between 62.00 and 73.20 wt % take place in the case of unbiodegraded copolymers and between 71.12–73.92 wt %, respectively, in the case of biodegraded ones. In the final stage of thermal decomposition (380°C–600°C), the weight losses range between 13.25 and 24.9 wt % in the case of unbiodegraded samples and between 12.20–18.6 wt % for biodegraded samples. Analyzing the thermal stability of PVA and copolymers according to weight losses of 10 and 50 wt %, respectively, it was ascertained that at the end of the biodegradation time the samples had a better thermal stability (Table III). It can be noticed that the T_{10} temperatures, where the weight losses are 10 wt % for unbiodegraded and biodegraded samples, respectively, are the following: 257°C and 260°C (for PVA), 219°C and 270°C (for PVA-g-LA, 1/1), 267°C and 270°C (for PVA-g-LA, 2.2/1). Also, the same thermal stability was ascertained and in the case of weight losses of 50 wt % (T_{50}), demonstrating that these thermal characteristics are influenced by PVA/LA molar ratio (the thermal stability is more raised in the case of the copolymer with molar ratio 2.2/1). The higher thermal stability of the biodegraded samples, demonstrate that

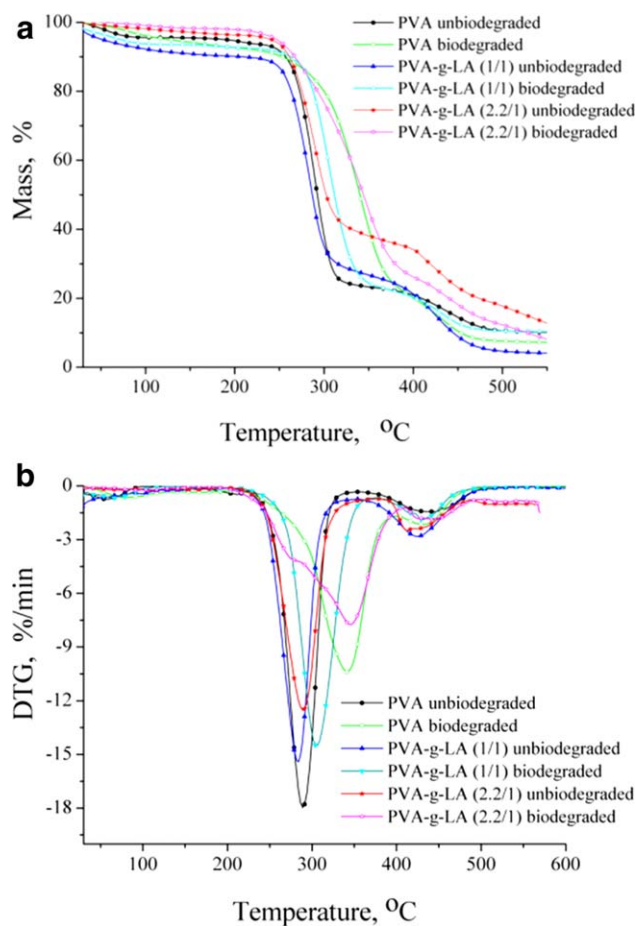


Figure 7. TG curves (a) and DTG curves (b) of PVA and PVA-g-LA copolymers unbiodegraded and biodegraded (24 days by *Trichotecium roseum* fungus). [Color figure can be viewed in the online issue, which is available at wileyonlinelibrary.com.]

Table III. Thermogravimetric Data for PVA and PVA-g-LA Copolymers Before and After 24 Days of Biodegradation by *Trichotecium roseum* Fungus

Sample	Degradation stage	T_{onset} (°C)	T_{peak} (°C)	T_{endset} (°C)	W (%)	T_{10} (°C)	T_{50} (°C)
PVA (blank)	I	46	57	93	4.55	257	293
	II	258	298	317	72.40		
	III	384	436	499	13.25		
	residue				9.80		
PVA biodegraded	I	51	85	128	6.02	260	347
	II	297	347	382	73.92		
	III	414	438	482	13.20		
	residue				6.86		
PVA-g-LA (1/1) (blank)	I	50	-	115	6.80	219	296
	II	255	292	317	73.20		
	III	387	434	495	16.75		
	residue				3.25		
PVA-g-LA (1/1) biodegraded	I	66	72	102	6.45	270	318
	II	276	312	349	71.12		
	III	411	438	479	12.20		
	residue				10.23		
PVA-g-LA (2.2/1) (blank)	I	80	-	220	3.20	267	311
	II	255	298	325	62.00		
	III	403	421	479	24.90		
	residue				8.90		
PVA-g-LA (2.2/1) biodegraded	I	70	-	200	2.00	270	345
	II	303	348	385	73.00		
	III	415	444	484	18.60		
	residue				6.40		

10°C/min, N₂, Al₂O₃, 30°C–600°C; T_{onset} , the temperature at which the thermal decomposition begins; T_{peak} , the temperature at which the degradation rate is maximum; T_{endset} , the temperature at end of the process; T_{10} , T_{50} , the temperature corresponding to 10 and 50 wt % weight loss; W, weight loss.

by biodegradation, the amorphous domains of PVA and PVA-g-LA copolymers were destroyed, the crystallinity degree increased and the remained macromolecular chains with more raised average molecular weight are more difficult thermally degraded (the result is in accordance with the DSC results).

CONCLUSIONS

This study investigated the ability of *T. roseum* fungus to grow and degrade PVA and PVA-g-LA copolymers. The clear zone technique showed that the fungal attack was faster in the case of copolymers with more lactic acid grafted units (molar ratio PVA/LA, 1/1), after six biodegradation days. The fungal attack on PVA was more reduced, comparatively to the studied copolymers, as demonstrated by the clear zone technique. The FTIR-ATR spectroscopy concluded that PVA structure was not very much modified after 24 days of biodegradation with this fungal species, but in PVA-g-LA copolymers the ester groups were destroyed after the same biodegradation period. The SEM studies demonstrated that for all studied samples, an abundant growth of fungi was observed at the end of the biodegradation time (24 days), the samples surface was covered with hyphae at a rate of 70%–90%.

The SLS analysis suggested that by biodegradation, the molecular weight of the copolymers and PVA increased, as the fractions with low molecular weight were destroyed. Also, the thermal stability of the biodegraded PVA and copolymers was more raised comparatively to the unbiodegraded ones, this result showed that the amorphous domains were destroyed, the crystallinity degree increased and the remained macromolecular chains with more raised average molecular weight are more difficult thermally degraded. Consequently, the studied PVA-g-LA copolymers are biodegradable in the presence of *T. roseum* fungus, are environmentally friendly and could be utilized in packaging, agriculture, biomedical, and pharmaceutical applications.

ACKNOWLEDGMENTS

The authors are grateful for the financial support from the Romanian National Authority for Scientific Research CNCS–UEFISCDI, project: Bionanomed: Antimicrobial bionanocomposites for medical applications, Grant PCCA/II, no 164/2012 and project: Interdisciplinary research on multifunctional hybrid particles for bio-requirements “INTERBIORES” PN-II–PT–PCCA–2011–3.2–0428, Grant no. 211/2012.

REFERENCES

1. Amass, W.; Amass, A.; Tighe, B. *Polym. Int.* **1998**, *47*, 89.
2. Gnanavel, G.; Mohana Jeya Valli, V. P.; Thirumarimurugan, M.; Kannadasan, T. *Int. J. Pharm. Chem. Sci.* **2013**, *1*, 691.
3. Navarchian, A. H.; Sharafi, A.; Kermanshahi, R. K. *J. Polym. Environ.* **2013**, *21*, 233.
4. Acemoglu, M. *Int. J. Pharm.* **2004**, *277*, 133.
5. Anderson, J. M.; Shive, M. S. *Adv. Drug. Deliv. Rev.* **1999**, *28*, 5.
6. Kale, G.; Kijchavengkul, T.; Auras, R.; Rubino, M.; Selke, S. E.; Singh, S. P. *Macromol. Biosci.* **2007**, *7*, 255.
7. Finch, C. A. *Polyvinyl Alcohol*; Wiley: New York, **1992**.
8. Tudorachi, N.; Chiriac, A. P. *J. Polym. Environ.* **2011**, *19*, 546.
9. Rojas Oviedo, I.; Noguez Mendez, N. A.; Gomez, M. P.; Cardenos Rodriguez, H.; Rubio Martinez, A. *Int. J. Polym. Mater. Polym. Biomater.* **2008**, *57*, 1095.
10. Taghizadeh, M. T.; Sabouri, N.; Ghanbarzadeh, B. *Springer Plus* **2013**, *2*, 376.
11. Argade, A. B.; Peppas, N. A. *J. Appl. Polym. Sci.* **1998**, *70*, 817.
12. Guerrouani, N.; Mas, A.; Schue, F. *J. Appl. Polym. Sci.* **2009**, *113*, 1188.
13. Tudorachi, N.; Lipsa, R. *J. Appl. Polym. Sci.* **2011**, *122*, 1109.
14. Tudorachi, N.; Lipsa, R. *Polimery* **2010**, *55*, 562.
15. Leja, K.; Lewandowicz, G. *Polish J. Environ. Stud.* **2010**, *19*, 255.
16. Solaro, R.; Corti, A.; Chiellini, E. *Polym. Adv. Technol.* **2000**, *11*, 873.
17. Tokiwa, Y.; Calabria, B. P. *J. Polym. Environ.* **2007**, *15*, 259.
18. Kim, M.; Kim, H.; Jin, H.; Park, J.; Yoon, J. *Eur. Polym. J.* **2001**, *37*, 1843.
19. Wang, N.; Yu, J. G.; Ma, X. F. *Polym. Int.* **2007**, *56*, 1440.
20. Torres, A.; Li, S. M.; Roussos, S.; Vert, M. *Appl. Environ. Microbiol.* **1996**, *62*, 2393.
21. Constantinescu, O. *Methods and Techniques in Mycology*; Ceres Ed: Bucharest, **1974**, pp 1–100.
22. Summerbell, R. C.; Gueidan, C.; Schroers, H. J.; de Hoog, G. S.; Starink, M.; Rosete, Y. A.; Guarro, J.; Scott, J. A. *Stud. Mycol.* **2011**, *68*, 139.
23. Cangemi, J. M.; dos Santos, A. M.; Neto, S. C.; Chierice, G. O. *Polimeros* **2008**, *18*, 201.
24. Tsujiyama, S.; Nitta, T.; Maoka, T. *J. Biosci. Bioeng.* **2011**, *112*, 58.
25. Karlsson, S.; Albertsson, A.-C. *Polym. Eng. Sci.* **1998**, *38*, 1251.
26. Flemming, H.-C. *Polym. Degrad. Stabil.* **1998**, *59*, 309.
27. Stoica-Guzun, A.; Jecu, L.; Gheorghe, A.; Raut, I.; Stroescu, M.; Ghiurea, M.; Danila, M.; Jipa, I.; Fruth, V. *J. Polym. Environ.* **2011**, *19*, 69.
28. Tuominen, J.; Kylma, J.; Kapanen, A.; Venelampi, O.; Itaavara, M.; Seppala, J. *Biomacromolecules* **2002**, *3*, 445.
29. Bos, R.; van der Mei, H. C.; Busscher, H. J. *FEMS Microbiol. Rev.* **1999**, *23*, 179.
30. Grigoraş, A. G.; Constantin, M.; Grigoraş, V. C.; Dunca, S. I.; Ochiuz, L. *React. Funct. Polym.* **2013**, *73*, 1249.
31. Podzimek, S. In *Light Scattering, Size Exclusion Chromatography and Asymmetric Flow Field Flow Fractionation. Powerful Tools for Characterization of Polymers, Proteins and Nanoparticles*; John Wiley and Sons Inc.: Hoboken, New Jersey, **2011**.
32. Carlfors, J.; Rymden, R. *Eur. Polym. J.* **1982**, *18*, 933.
33. Czechowska-Biskup, R.; Wojtasz-Paiak, A.; Sikorski, J.; Henke, A.; Ulanski, P.; Rosiak, J. M. *Polish Chitin Society Monograph XII* **2007**, 87–94.
34. Bohlman, G. M. General Characteristics, Processability, Industrial Applications and Market Evolution of Biodegradable Polymers; In *Handbook of Biodegradable Polymers*; Bastioli, C., Eds; Rapra Technology Limited: Shropshire, UK, **2005**.
35. Tokiwa, Y.; Calabria, B. P.; Ugwu, C. U.; Aiba, S. *Int. J. Mol. Sci.* **2009**, *10*, 3722.
36. Jeon, H. J.; Kim, M. N. *Biodegradation* **2013**, *24*, 89.